Human Molecular Genetics, 2019, Vol. 28, No. 17 2937–2951

doi: 10.1093/hmg/ddz117
Advance Access Publication Date: 15 May 2019
General Article

GENERAL ARTICLE

De novo loss-of-function *KCNMA1* variants are associated with a new multiple malformation syndrome and a broad spectrum of developmental and neurological phenotypes

Lina Liang[1,†], Xia Li[1,18,†], Sébastien Moutton[2,3,4,†], Samantha A. Schrier Vergano[5,†], Benjamin Cogné[6,†], Anne Saint-Martin de[7,†], Anna C. E. Hurst[8,†], Yushuang Hu[1,†], Olaf Bodamer[9,10,†], Julien Thevenon[2,3,4,†], Christina Y. Hung[9,†], Bertrand Isidor[6,†], Bénédicte Gerard[11,†], Adelaide Rega[12], Sophie Nambot[2,3,4], Daphné Lehalle[2,3,4], Yannis Duffourd[2,3,4], Christel Thauvin-Robinet[2,3,4], Laurence Faivre[2,3,4], Stéphane Bézieau[6], Leon S Dure[13], Daniel C. Helbling[14], David Bick[14], Chengqi Xu[1], Qiuyun Chen[15], Grazia M.S. Mancini[16,*], Antonio Vitobello[4,*] and Qing Kenneth Wang[1,15,17,*]

[1]Key Laboratory of Molecular Biophysics of the Ministry of Education, College of Life Science and Technology, Center for Human Genome Research, Cardio-X Institute, Huazhong University of Science and Technology, Wuhan, Hubei 430074, P. R. China, [2]Centre de Référence Anomalies du Développement et Syndromes Malformatifs, Hôpital d'Enfants, Dijon 21079, France, [3]Centre de Référence Déficiences Intellectuelles de Causes Rares, Hôpital d'Enfants, Dijon 21079, France, [4]Inserm UMR 1231 GAD team, Genetics of Developmental Disorders, Université de Bourgogne Franche-Comté, Dijon 21070, France, [5]Medical Genetics and Metabolism, Children's Hospital of The King's Daughters, Eastern Virginia Medical School, Norfolk, VA 23507, USA, [6]Service de Génétique Médicale, CHU de Nantes, Nantes 44093, France, [7]Neuropédiatrie, Centre de Référence des Epilepsies Rares, Hôpitaux Universitaires de Strasbourg, Strasbourg 67098, France, [8]Department of Genetics, University of Alabama at Birmingham, Birmingham, AL 35294, USA, [9]Division of Genetics and Genomics, Boston Children's Hospital/Harvard Medical School, Boston, MA 02115, USA, [10]The Broad Institute of Harvard and MIT, Boston, MA 02115, USA, [11]Institut de Génétique Médicale d'Alsace, Laboratoires de Diagnostic Génétique, Unité de Génétique Moléculaire, Nouvel Hôpital Civil, Strasbourg 67000, Franc, [12]Pediatric Radiologist, Département de Radiologie et Imagerie Diagnostique et Thérapeutique, CHU, Dijon 21079, France, [13]Department of Pediatrics and Neurology, University of Alabama at Birmingham, Birmingham, AL 35233, USA, [14]Clinical Services Laboratory, HudsonAlpha Institute for Biotechnology, Huntsville, AL 35806, USA,

[†]These authors contributed equally to this work.

Received: February 4, 2019. **Revised:** April 17, 2019. **Accepted:** May 21, 2019

[15]Department of Cardiovascular and Metabolic Sciences, Lerner Research Institute, Department of Cardiovascular Medicine, Cleveland Clinic, Department of Molecular Medicine, Cleveland Clinic Lerner College of Medicine of Case Western Reserve University, Cleveland, OH 44195, USA, [16]Department of Clinical Genetics, Erasmus University Medical Center, Rotterdam 3015, The Netherlands, [17]Department of Genetics and Genome Science, Case Western Reserve University School of Medicine, Cleveland, OH 44106, USA and [18]Present address: Life Sciences Institute, University of Michigan, Ann Arbor, MI 48109, USA

*To whom correspondence should be addressed at: Qing Kenneth Wang, Department of Cardiovascular and Metabolic Sciences, Lerner Research Institute, Cleveland Clinic, 9500 Euclid Ave, Cleveland, OH 44195, USA and Center for Human Genome Research, HUST, Wuhan 430074, China. Tel: (216) 4450570; Fax: (216) 4458204; Email: wangq2@ccf.org or qkwang@hust.edu.cn; Antonio Vitobello, Genetics of Developmental Disorders, Université de Bourgogne Franche-Comté, Dijon 21070, France. Tel: 03 80 39 32 38; Fax: 03 80 29 32 66; Email: Antonio.Vitobello@u-bourgogne.fr; Grazia Mancini, Department of Clinical Genetics, Erasmus University Medical Center, Rotterdam 3015, The Netherlands. Tel: 31-10-7036915; Fax: 31-10-7043072; Email: g.mancini@erasmusmc.nl

Abstract

KCNMA1 encodes the large-conductance Ca^{2+}- and voltage-activated K^+ (BK) potassium channel α-subunit, and pathogenic gain-of-function variants in this gene have been associated with a dominant form of generalized epilepsy and paroxysmal dyskinesia. Here, we genetically and functionally characterize eight novel loss-of-function (LoF) variants of *KCNMA1*. Genome or exome sequencing and the participation in the international Matchmaker Exchange effort allowed for the identification of novel *KCNMA1* variants. Patch clamping was used to assess functionality of mutant BK channels. The *KCNMA1* variants p.(Ser351Tyr), p.(Gly356Arg), p.(Gly375Arg), p.(Asn449fs) and p.(Ile663Val) abolished the BK current, whereas p.(Cys413Tyr) and p.(Pro805Leu) reduced the BK current amplitude and shifted the activation curves toward positive potentials. The p.(Asp984Asn) variant reduced the current amplitude without affecting kinetics. A phenotypic analysis of the patients carrying the recurrent p.(Gly375Arg) *de novo* missense LoF variant revealed a novel syndromic neurodevelopmental disorder associated with severe developmental delay, visceral and cardiac malformations, connective tissue presentations with arterial involvement, bone dysplasia and characteristic dysmorphic features. Patients with other LoF variants presented with neurological and developmental symptoms including developmental delay, intellectual disability, ataxia, axial hypotonia, cerebral atrophy and speech delay/apraxia/dysarthria. Therefore, LoF *KCNMA1* variants are associated with a new syndrome characterized by a broad spectrum of neurological phenotypes and developmental disorders. LoF variants of *KCNMA1* cause a new syndrome distinctly different from gain-of-function variants in the same gene.

Introduction

The large-conductance Ca^{2+}- and voltage-activated K^+ (BK) channel is a tetramer consisting of four α-subunits encoded by the *KCNMA1* gene on chromosome 10q22.3. Each α-subunit spans 1236 amino acids and has an estimated molecular weight of 138 kDa (1–3). The α-subunit contains seven transmembrane domains (S0–S6) at its N terminus and a large C-terminal domain comprising of two RCK domains (regulator of conductance of K domains RCK1 and RCK2) responsible for calcium sensing through a high-affinity Ca^{2+} binding site (2,3). The S4 domain acts as the voltage sensor, and a region between S5 and S6 serves as the pore (2,3). The BK channel has a tetrameric structure composed of four pore-forming α-subunits, in which the four RCK1-RCK2 tandems form the 'gating ring' structure that is believed to interact with the voltage-sensing region, leading to the opening of the pore (2,3). The BK channel can be allosterically activated by both changes in the membrane voltage (voltage-dependent activation pathway) and intracellular [Ca^{2+}] concentration (calcium-dependent activation pathway) (2,3). The physiological properties of BK channels are further influenced by the interaction of their α-subunits with optional auxiliary subunits such as β1–4 subunits or γ1–4 subunits (2,3).

The BK channel is expressed in many organs and tissues, including the postnatal central nervous system (2,3). It plays a pleiotropic role in many physiological processes, such as in the repolarization of the membrane potential, the control of neuronal excitability, neurotransmitter release, the control of smooth muscle tone, the tuning of hair cells in the cochlea and in innate immunity (4–8). Recently, the BK channel was found to be involved in the maintenance, migration and differentiation of mesenchymal stromal cell populations and in the SH-SY5Y neuroblastoma cell cycle and proliferation (9,10).

In 2005, BK channel abnormalities were linked to human disease for the first time through the identification of a *KCNMA1* gain-of-function mutation, which causes a coexistent syndrome of generalized epilepsy and paroxysmal dyskinesia (GEPD) (1). By genome-wide linkage analysis of a large family with 13 affected individuals and through subsequent DNA sequence analyses, Du *et al.* (1) had found the p.(Asp434Gly) pathogenic variant in *KCNMA1*, which co-segregated with GEPD in the family. Patch-clamping studies showed that the p.(Asp434Gly) mutation increased the BK current by enhancing channel activation and increasing the calcium sensitivity of the BK channel (1). Recently, Li *et al.* (11) identified a *de novo KCNMA1* variant p.(Asn995Ser) in two independent patients who presented with epilepsy but not with paroxysmal dyskinesia. The p.(Asn995Ser) variant also increased the BK current by enhancing the BK channel activation through increases in the single-channel open probability and single-channel open dwell time. However, the variant did not alter the calcium sensitivity of the channel (11). As both p.(Asp434Gly) and p.(Asn995Ser) variants enhance the BK channel current and activation, they elicit a

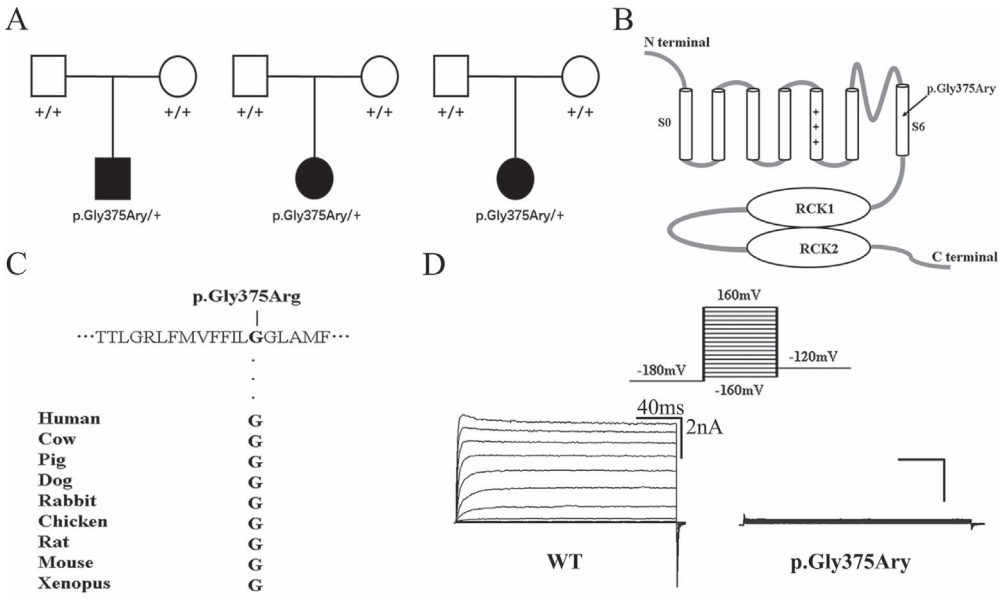

Figure 1. Identification and electrophysiological characterization of a recurrent *de novo KCNMA1* variant p.(Gly375Arg) in the transmembrane segment S6 of the BK channel. (**A**) Pedigree of three families with genotyping data for the *KCNMA1* variant p.(Gly375Arg) showing the *de novo* nature of the variant. The affected male and females are shown as filled squares or circles. Normal individuals are shown as empty symbols. (**B**) Schematic structure of the BK channel. The location of the p.(Gly375Arg) variant is indicated by an arrow. (**C**) The p.(Gly375Arg) variant occurs at an evolutionally conserved amino acid residue. (**D**) Electrophysiological characterization of the p.(Gly375Arg) variant. Representative macroscopic currents of WT and p.(Gly374Arg) mutant BK channels from inside-out patch experiments in the presence of 10 μM Ca^{2+} using the protocol indicated at the top ($n = 6$–10/group).

gain-of-function effect (1,11). Tabarki *et al.* (12) reported two Saudi sisters with epilepsy, developmental delay and severe cerebellar atrophy carrying a homozygous 1 bp duplication [c.2026dupT, p.(Tyr676Leufs*7)] in *KCNMA1*. The variant was seen once in the Exome Aggregation Consortium (ExAC) database but was absent from the Genome Aggregation Database (gnomAD). No functional studies of the variant were performed. Zhang *et al.* (13) reported two Chinese boys with paroxysmal non-kinesigenic dyskinesia and developmental delay without generalized epilepsy but *de novo* heterozygous p.(Glu884Lys) and p.(Asn1053Ser) variants in *KCNMA1*, respectively. Functional studies of these variants were not performed. Li *et al.* (11) reported three additional *KCNMA1* variants p.(Lys518Asn), p.(Asp656Ala) and p.(Asn1159Ser) in three unrelated patients with divergent epileptic phenotypes. However, functional studies established the variants as benign polymorphisms, indicating the necessity of functional characterization of *KCNMA1* variants for accurate variant classification.

Here, we report both genetic and functional analyses of eight novel *KCNMA1* variants, including six *de novo* variants, which were detected in eight unrelated patients and two compound heterozygous variants found to be present in one patient. Electrophysiological data suggest that all variants act through a loss-of-function (LoF) mechanism. Therefore, this study expands the mutational spectrum of *KCNMA1*-related disorders and describes a new clinical entity elicited by the recurrent LoF variant p.(Gly375Arg). This new syndrome is associated with developmental delay, visceral and cardiac malformations, epilepsy, connective tissue symptoms with arterial involvement, bone dysplasia and characteristic dysmorphic features in three independent patients. Furthermore, this research offers comprehensive functional analyses of the largest cohort of BK channel LoF variants and reveals the novel pathogenic potential of *KCNMA1* LoF variation in human disease.

Results

Identification of a new syndrome associated with a recurrent *de novo* missense variant in *KCNMA1*

Exome sequencing identified a *de novo KCNMA1* missense variant [NM_002247.3: c.1123G>A, p.(Gly375Arg)] in three unrelated families (Fig. 1A). The p.(Gly375Arg) variant is located in the S6 transmembrane domain of the BK channel (Fig. 1B) and occurs at an amino acid residue, which is highly conserved among different species during evolution (Fig. 1C). This variant is absent from gnomAD and has a single submission as a VUS (variant of uncertain significance) in both ClinVar (RCV000623526.1) and the denovo-db database (denovo-db.gs.washington.edu, sample DDD4K.008888, associated with developmental disorder). Patch-clamping experiments revealed that the p.(Gly375Arg) variant abolishes the function of the BK channel and blocks generation of potassium current (Fig. 1D), suggesting a LoF effect of this variant.

The p.(Gly375Arg) variant was first identified in a 2-year-old boy (Patient 1 in Table 1 and Supplementary Material, Fig. S1) presenting with a polymalformation syndrome characterized by severe developmental delay, visceral and cardiac malformations, connective tissue symptoms with arterial involvement, generalized seizures and dysmorphic features including coarse facial features, macroglossia with two-lobed tongue, gingival hypertrophy, synophrys, hypertelorism, down-slanting palpebral fissures, broad nasal root, thin superior lip, wide mouth with downturned corners, everted lower lip, frontal hemangioma, mild hirsutism and skin infiltrations. Strabismus and vertical nystagmus were also noted at clinical examinations (Table 1). At the age of 3 years and 4 months, his sitting position was still unstable/unsteady. He could walk some steps with support, the tone progressively improved, the sleep quality was better after amygdala and adenoid surgery improved babbling at the

same time. There was no feeding difficulty. At the age of 3 years and 6 months, snoring recurrence, decreased vocal production and tonsil hypertrophy led to another amygdala and adenoid surgery. In the post-surgery period, it was not possible to remove ventilation support due to severe laryngomalacia. Five days after the surgery, he presented with degradation of respiratory functions, occlusive syndrome and oligo-anuria. Palliative measures were established in accordance with parent's choice and after approval of the local ethics committee. He deceased at the sixth day after surgery.

Similar clinical features were observed in a second unrelated patient (Patient 2 in Table 1 and Supplementary Material, Fig. S1), who was previously identified to carry the same p.(Gly375Arg) variant by singleton exome sequencing by the same diagnostic laboratory. Subsequent Sanger sequencing revealed the *de novo* occurrence of this variant also in Patient 2. She is a 27-year-old female patient, who has been followed since birth for developmental delay, intellectual disability (ID), speech delay, severe axial hypotonia, mild cerebellar and cerebral atrophy identified by magnetic resonance imaging (MRI), absence epilepsy, megalocornea, intestinal atresia and malrotation, patent ductus arteriosus and dysmorphic features (Table 1). Patients 1 and 2 have undergone multiple imaging studies [X-rays, computer tomography (CT) scans and brain MRIs] during their clinical care, which show generalized bone thickening, sclerosis and dysplasia, bowel loop dilatation during episodes of intestinal pseudoobstruction, and dilatation, ectasia and tortuosity of large and medium-sized arteries in both individuals (Table 1; Supplementary Material, Fig. S2). A medical record review of Patient 2 identified additional clinical symptoms such as chronic *Staphylococcus epidermidis* bacteremia and frequent fevers. A CT scan at age 26 years documented hepatomegaly (20 cm), splenomegaly (17 cm) and several vertebrae collapses (Table 1; Supplementary Material, Fig. S2). A cardiac ultrasound at age 26 years measured an enlarged ascending aorta diameter of 38–39 mm with no evidence of an infectious endocarditis (Table 1). Through the international Matchmaker Exchange initiative (14), we identified one additional unrelated female patient bearing the same *de novo* p.(Gly375Arg) variant who presented with an overlapping phenotype (Patient 3 in Table 1; Supplementary Material, Fig. S1). Together, these data suggest that this recurrent *de novo* p.(Gly375Arg) LoF variant of *KCNMA1* is associated with a multiple malformation syndrome.

De novo variants in the pore domain also abolish BK channel function

Two additional *de novo* missense variants, p.(Ser351Tyr) and p.(Gly356Arg), were identified in the pore domain of the BK channel (Fig. 2A and B). Patient 4, who carries the p.(Ser351Tyr) variant, is a 10-year-old female patient with ataxia, tremor, apraxia, hypertelorism, bilateral medial deviation of the distal phalanges of the third finger and lateral deviation of the toes (Table 1; Supplementary Material, Fig. S3). Brain MRI did not detect any structural abnormalities in this individual. She is not affected by seizures or paroxysmal dyskinesia (Table 1). Patient 5 carries the p.(Gly356Arg) variant and is a 12-year-old male affected by mild cognitive delay, axial hypotonia, ataxia and dysarthria (Table 1). Serial MRI detected cerebellar atrophy. The patient does not exhibit epilepsy.

Both p.(Ser351Tyr) and p.(Gly356Arg) variants occur at amino acid residues, which are highly conserved among different species and are located in a motif important for the selectivity for potassium (Fig. 2C). Patch-clamp recordings showed that BK channels with either p.(Ser351Tyr) or p.(Gly356Arg) variants fail to elicit any potassium current under voltage stimulus ranging from −160 mV–160 mV (Fig. 2D). These data suggest that the p.(Ser351Tyr) and p.(Gly356Arg) variants are also LoF variants.

Electrophysiological characterization of compound heterozygous variants p.(Asn449fs) and p.(Cys413Tyr) identified in a patient

We identified two compound heterozygous variants in a patient (Patient 6 in Table 1). Both, the maternally inherited missense variant p.(Cys413Tyr) and the frameshift variant p.(Asn449fs), which is inherited from the father, are located in the C-terminal RCK1 domain (Fig. 3A and B) important for the regulation of K conductance. The patient presented with multiple congenital abnormalities, developmental delay, ID, axial hypotonia, ataxia, generalized mild cerebral atrophy documented by MRI and strabismus (Table 1). Both parents are clinically asymptomatic at the present time. The p.(Cys413Tyr) variant occurs at an amino acid residue, which is highly conserved among different species during evolution (Fig. 3C), and markedly reduces the amplitude of the BK current and shifts the G-V curve to the positive voltage direction by 38 mV at the 10 μM calcium concentration (Fig. 3D). The mean macroscopic current amplitude of the p.(Cys413Tyr) mutant channel was much smaller than that of the wild-type (WT) channels ($n = 11$ for mutant and $n = 6$ for WT) (Fig. 3D). Thus, the p.(Cys413Tyr) variant is also a LoF variant that inhibits the function of the BK channel substantially. To test the calcium dependency of the p.(Cys413Tyr) mutant channel, we further analyzed the G-V relationship at 1 μM and nominal 0 μM calcium concentrations and found that the G-V curves of the mutant channels also shifted to the positive voltage direction by 26.2 mV and 33.7 mV, respectively (Fig. 3D). Thus, the p.(Cys413Tyr) variant likely reduces the activation and macroscopic current amplitude of the BK channel significantly at calcium concentrations ranging from nominal 0 μM–10 μM.

The frameshift variant p.(Asn449fs) did not elicit any potassium current under the voltage stimulus from −160 mV–160 mV at a 10 μM calcium concentration (Fig. 3D). These data suggest that the p.(Asn449fs) variant is also a LoF variant.

De novo variant p.(Ile663Val) in the RCK1 domain abolishes the function of the BK channel

KCNMA1 variant p.(Ile663Val) was identified in a female patient (Patient 7) who suffers from developmental delay, ID, axial hypotonia, ataxia and strabismus (Table 1). The variant was found to occur *de novo* and is located in the RCK1 domain of the BK channel (Fig. 4A and B). This substitution occurs at an amino acid residue, which is highly conserved among different species during evolution (Fig. 4C). Patch-clamp recordings showed that p.(Ile663Val) mutant BK channels failed to elicit any potassium current under the voltage stimulus from −160 mV–160 mV (Fig. 4D). Interestingly, western blot analyses revealed that the p.(Ile66Val) mutated BK channel moved much slower than the WT or other mutant channels through the gel (Fig. 4E). The 3D structure of the BK channel shows that the amino acid Ile663 is a hydrophobic residue buried inside the structure. Thus, the substitution of isoleucine by valine at codon 663 may alter the 3D structure of the BK channel dramatically, which may explain the altered migration pattern on the western blot. These data suggest that the p.(Ile663Val) variant is a functional variant, which leads to LoF of the BK channel.

Table 1. Clinical data of nine patients with eight different LoF variants in BK channels

Patient ID	4	5	1	2	3	6	7	8	9
Genomic variant	p.Ser351Tyr	p.Gly356Arg	p.Gly375Arg	p.Gly375Arg	p.Gly375Arg	p.Asn449fs/ p.Cys413Tyr	p.Ile663Val	p.Pro805Leu	p.Asp984Asn
De novo variant	Yes	Yes	Yes	Yes	Yes	No	Yes	Yes	Yes
Consanguinity	No	No	No	No	No	No	No	No	No
Gender	F	M	M	F	F	M	F	M	M
Gestational Age (WG)	40 + 1/7 w	At term	36 w	37 w	40 w	At term (40 + 4/7 w)	NA	40 w	40 w
Birth parameters									
Weight	3.2 kg (30%)	NA	3.80 kg (98%)	2.95 kg (50%)	3.97 kg (93%)	3.640 kg (60%)	2.55 kg	5.58 kg (99.9%)	2.13 kg (0.1%)
Length	53 cm (90%)	NA	48 cm (55%)	50 cm (85%)	48.5 cm (36%)	NA	NA	55 cm (99%)	50 cm (30%)
OFC	NA	NA	35 cm (85%)	33.5 cm (50%)	35 cm (83%)	NA	NA	35.5 cm (55%)	34 cm (20%)
Growth parameters (age)	10 y	10 y	3 y 4 m	21 y	12 y	2 y	3 y 10 m	4 y	4 y
Weight	32.3 kg (39%)	90%	13 kg (20%)	46 kg (25%)	26.7 kg (0.4%)	75%	12.2 kg (5%)	35.1 kg (99.99%)	19.3 kg (97.5%)
Height	138 cm (42%)	75%	93 cm (30%)	151 cm (2.5%)	136 cm (2.12%)	75%	92 cm (5%)	117.3 cm (99.9%)	109 cm (97.5%)
OFC	53 cm (62%)	50%	50 cm (45%)	56 cm (15%)	NA	50%	46.5 cm (0.1%)	52.4 cm (80%)	50 cm (70%)
Facial dysmorphism	Yes	No	Yes	Yes	Yes	Mild brachy-cephalic	No	No	No
Synophrys	−		+	−	−	−			
Hypertelorism	+ (Inner canthus 95%ile)		+	+	+	−			
Down-slanting palpebral fissures	−		+	+	+	+ (Short palpebral fissures, epicanthic folds)			
Broad nasal root	−		+	+	(+)	+			

(Continued)

Table 1. Continued

Patient ID Genomic variant	4 p.Ser351Tyr	5 p.Gly356Arg	1 p.Gly375Arg	2 p.Gly375Arg	3 p.Gly375Arg	6 p.Asn449fs/ p.Cys413Tyr	7 p.Ile663Val	8 p.Pro805Leu	9 p.Asp984Asn
Thin superior lip	−		+	+	(+)	+			
Wide mouth with downturned corners	−		+	+	−	−			
Prominent incisors	−		NA	NA	+	−			
Diastemas of the teeth	−		NA	NA	+	−			
Everted inferior lip	−		+	No	+	−			
Visceral malformations	No	No	Severe aortic root dilatation, omphalocele, megabladder	Moderate aortic root dilatation, common mesentery, umbilical hernia	Mild aortic root dilatation megacystis	No	No	Obesity	No
Eye/hearing features	No	No	Strabismus, nystagmus	Megalocornea	No	Strabismus	Strabismus/right macular coloboma, left sensorineural deafness	No	No
Neurological/ developmental features									
Sitting age	8 m	8.5 y	NA	2 y	2.5 y	NA	NA	Unknown	7 m
Walking age	20 m	NA	NA	NA	No	NA	NA	15 m	12 m
Speech delay	Yes, apraxia	Yes, dysarthria, No ID: TIQ	NA	Yes	Few words	NA	24 m	Severe, apraxia	Severe
DD/ID	Mild	85, Yes	Severe	Severe	Severe	Yes	Yes	Yes	Yes
Axial hypotonia	Mild	No	Mild	Severe	Severe	Yes	NA	No	No
Dystonia	No	Yes +++	No	No	No	No	NA	No	No

(Continued)

Table 1. Continued

Patient ID	4	5	1	2	3	6	7	8	9
Genomic variant	p.Ser351Tyr	p.Gly356Arg	p.Gly375Arg	p.Gly375Arg	p.Gly375Arg	p.Asn449fs/ p.Cys413Tyr	p.Ile663Val	p.Pro805Leu	p.Asp984Asn
Ataxia	Yes	Spasticity of the lower extremi-ties	No	No	No	Yes	Yes	No	No
Others	Tremor, dysmetria		No	Areflexia	No	No (normal DTR)			Autistic features
Epilepsy details	No	No seizures, no EEG	No	Absence	Absence	No	NA	No	Generalized and focal dystonic seizures, status epilepticus
Anticonvulsant treatment		No		Sodium valproate (depakine)	Lamotrigine				CLB, ESM, LTG, ZNS, VPA, PB, LCM
Cerebral MRI	Normal	Progressive atrophy of cerebellar hemi-spheres and vermis	Normal	Mild cerebellar and cerebral atrophy	Normal	Generalized mild cerebral atrophy, thin corpus callosum, mild atrophy of cerebellar vermis	Normal	White matter signal abnormality frontal lobes, pineal cyst	Normal
EEG features	NA	NA	NA	Normal	Normal	Normal	NA	Normal	Variable foci Global EEG slowing

(Continued)

Table 1. Continued

Patient ID Genomic variant	4 p.Ser351Tyr	5 p.Gly356Arg	1 p.Gly375Arg	2 p.Gly375Arg	3 p.Gly375Arg	6 p.Asn449fs/ p.Cys413Tyr	7 p.Ile663Val	8 p.Pro805Leu	9 p.Asp984Asn
Additional clinical features	Medial deviation of the third finger distal phalange bilaterally. Lateral deviation of the toes (especially hallux) with toe 2 overlapping toe 3 bilaterally	No	Neonatal diabetes, laryngomalacia, feeding difficulties, kyphosis thick ribs	High-arched palate, short neck, hypertelorism, long and smooth philtrum, massive and progressive gingival hypertrophy, abnormal dental implantation, mandibular exostosis, macroglossia, abnormal bowel motility (frequent digestive occlusions, gastroparesis), recurrent pyelonephritis, bilateral valgus foot deformity, elbows flessum, genu valgum, dorsal kyphosis, fingers hyperlaxity and clitoral hypertrophy	Abnormal bowel motility (chronic use of flagyl), megacystis (diagnosed prenatally), recurrent urinary tract infections and chronic retention, gingival hyperplasia required four reduction surgeries	No	Congenital torticoli	No	No

DD means developmental delay; F, female; M, male; y, years; m, months; w, weeks; NA, data not available

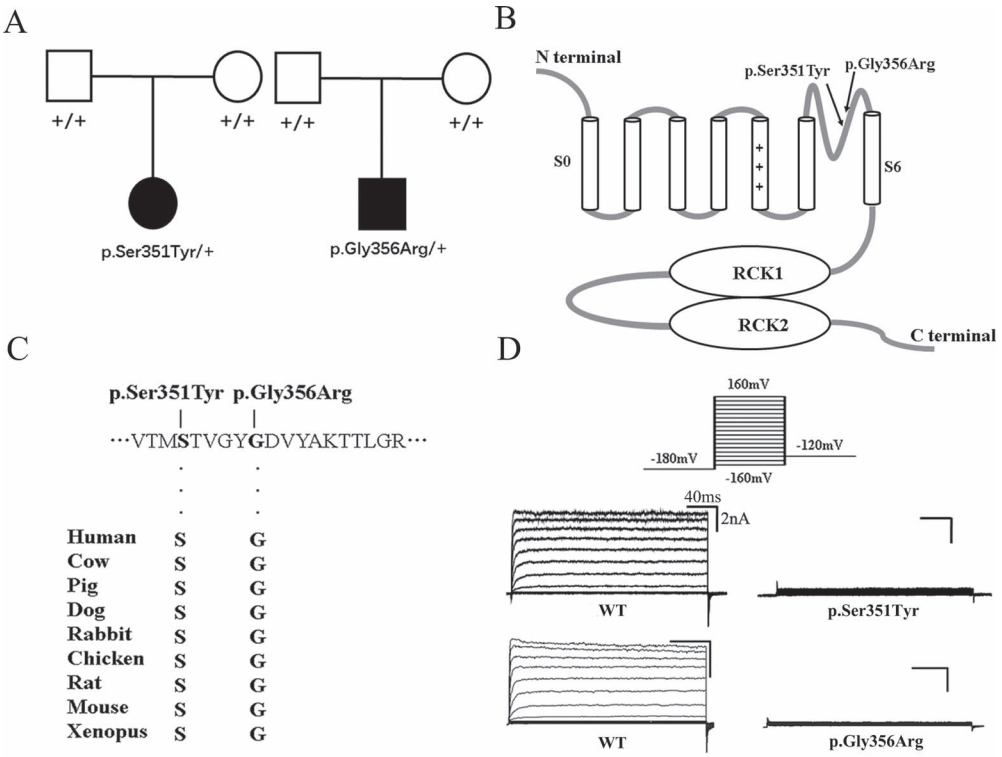

Figure 2. Identification and electrophysiological characterization of *KCNMA1* variants p.(Ser351Tyr) and p.(Gly356Arg) in the pore region of the BK channel. (**A**) Pedigree structure and genotyping data for each *KCNMA1* variant showing the *de novo* nature of the variants. (**B**) Schematic structure of the BK channel with the two variants indicated by arrows. (**C**) The two variants occur at an evolutionarily conserved amino acid residues. (**D**) Electrophysiological characterization of the two variants. Representative macroscopic currents of WT and mutant BK channels with p.(Ser351Tyr) and p.(Gly356Arg) from inside-out patch experiments in the presence of 10 μM Ca^{2+} using the protocol indicated at the top ($n = 6$–10/group).

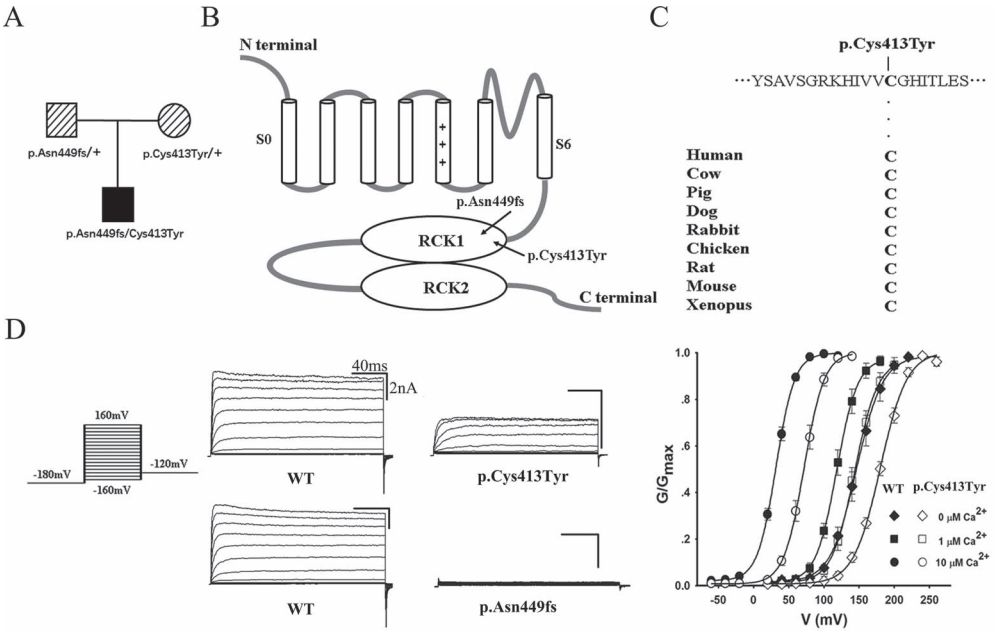

Figure 3. Identification and electrophysiological characterization of compound heterozygous *KCNMA1* variants p.(Asn449fs) and p.(Cys413Tyr) found in a patient. (**A**) Pedigree structure of the family and genotyping data for two *KCNMA1* variants. The affected male is shown as a filled square. Individuals with uncertain phenotype or without medical examination are shown as slashed symbols. (**B**) Schematic structure of the BK channel with the two variants in the RCK domains indicated with arrows. (**C**) The Cys413 residue occurs at an evolutionarily conserved amino acid residue. (**D**) Electrophysiological characterization of variants p.(Asn449fs) and p.(Cys413Tyr). Representative macroscopic currents of WT and mutant BK channels with p.(Asn449fs) and p.(Cys413Tyr) variants from inside-out patch experiments in the presence of 10 μM Ca^{2+} using the protocol indicated at the top. G-V curves of WT and p.(Cys413Tyr) mutant BK channels at nominal 0 μM Ca^{2+}, 1 μM Ca^{2+} and 10 μM Ca^{2+}. All G-V curves are fitted by Boltzmann function (solid lines) with $V_{1/2}$ and slope factor at nominal 0 μM Ca^{2+} [149.0 ± 9.5 mV, 17.9 ± 1.9 for WT and 182.7 ± 5.2 mV, 19.4 ± 2.0 for p.(Cys413Tyr)], at 1 μM Ca^{2+} [120.7 ± 11.2 mV, 14.7 ± 3.4 for WT and 146.9 ± 12.6 mV, 14.2 ± 2.5 for p.(Cys413Tyr)] and at 10 μM Ca^{2+} [31.7 ± 4.1 mV, 13.2 ± 1.3 for WT and 70.2 ± 9.6 mV, 12.6 ± 2.0 for p.(Cys413Tyr)]. The data are presented as mean ± SD ($n = 6$–11/group).

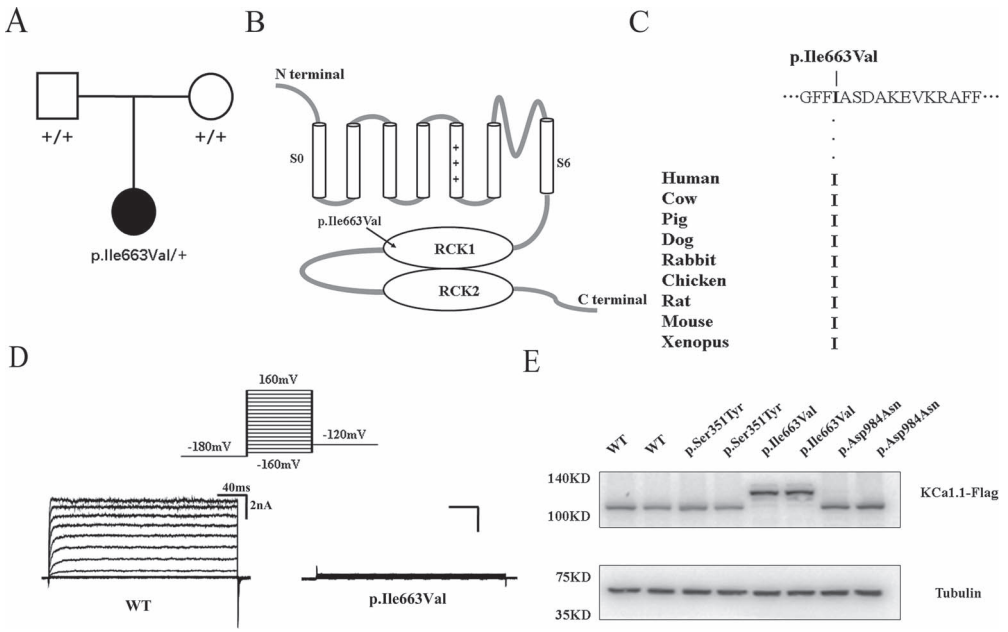

Figure 4. Identification and electrophysiological characterization of *KCNMA1* variant p.(Ile663Val) in the RCK1 domain of the BK channel. (**A**) Pedigree structure and genotyping data for *KCNMA1* variant p.(Ile663Val) showing the *de novo* occurrence of the variant. (**B**) Schematic structure of the BK channel with the location of variant p.(Ile663Val) indicated by an arrow. (**C**) The p.(Ile663Val) variant occurs at an evolutionarily conserved amino acid residue. (**D**) Electrophysiological characterization of variant p.(Ile663Val). Representative macroscopic currents of WT and p.(Ile663Val) mutant BK channels from inside-out patch experiments in the presence of 10 μM Ca^{2+} using the protocol indicated at the top ($n = 12–15$/group). (**e**) Western blot analysis showing that variant p.(Ile663Val) altered the mobility of the BK channel through SDS-polyacrylamide gels. Tubulin was used as a loading control.

De novo variants in the RCK2 domain markedly reduce the amplitude of the BK current

Two *KCNMA1* variants were identified at two evolutionarily highly conserved amino acid residues in the RCK2 domain of the BK channel (Fig. 5A–C). *KCNMA1* variant p.(Pro805Leu) was found *de novo* (Fig. 5A) in a male patient (Patient 8) presenting with severe speech delay, development delay, ID, apraxia and abnormal cerebral MRI (Table 1). The p.(Pro805Leu) variant markedly reduces the amplitude of the BK current (Fig. 5D). A western blot analysis showed that p.(Pro805Leu) significantly reduced the expression level of the BK channel (Fig. 5E). Moreover, the p.(Pro805Leu) variant shifts the G-V curve to the positive voltage direction (Fig. 5D) similar to p.(Cys413Tyr). Thus, the p.(Pro805Leu) variant is also a LoF variant.

KCNMA1 variant p.(Asp984Asn) is also a *de novo* variant (Fig. 5A), which was identified in a male patient (Patient 9) affected with non-syndromic moderate ID, severe language impairment, pharmacoresistant multifocal epilepsy but without paroxysmal dyskinesia (Table 1). The p.(Asp984Asn) variant occurs at an amino acid residue, which is highly conserved among different species during evolution (Fig. 5C). Patch-clamp recordings showed that the p.(Asp984Asn) variant markedly reduces the activation of the BK channel by decreasing the mean macroscopic current amplitude of BK potassium current (Fig. 5D). In contrast to the p.(Cys413Tyr) and p.(Pro805Leu) variants, the p.(Asp984Asn) variant does not alter the G-V curves (Fig. 5D). These data suggest that the p.(Asp984Asn) variant is a variant that leads to LoF of the BK channel.

Discussion

In this study, we identified and characterized eight LoF variants of *KCNMA1*, including p.(Ser351Tyr) and p.(Gly356Arg) in the pore region; p.(Gly375Arg) in the S6 transmembrane domain; p.(Asn449fs), p.(Cys413Tyr) and p.(Ile663Val) in RCK1; and p.(Pro805Leu) and p.(Asp984Asn) in RCK2. None of the variants have previously been reported in public databases such as the ExAC, gnomAD, 1000Genomes and Exome Variant Server. The p.(Gly375Arg) variant was reported once as VUS in ClinVar and in the denovo-db database (denovo-db.gs.washington.edu). All eight variants showed profound effects on BK channel function exerting their effects through a LoF mechanism (Fig. 1–5). This study presents in-depth functional electrophysiological characterization of the largest cohort of LoF variants identified in the BK channel to date. The deleterious effects of the eight identified variants on the BK channel suggest that the affected amino acid residues are indeed critical to the structure and function of the BK channel. In addition, the observed impairments of the BK channel function in the patch-clamping experiments on missense variants in RCK1 [p.(Cys413Tyr) and p.(Ile663Val)] as well as in RCK2 [p.(Pro805Leu) and p.(Asp984Asn)] suggest that both domains (RCK1 and RCK2) are critical to the generation and conductance of BK potassium currents.

Among patients with LoF variants in the BK channel, six patients shared the clinical features of ID and developmental delay, four individuals presented with ataxia and axial hypotonia and three affected were found to have cerebral atrophy (Table 1). These neurological and developmental abnormalities may be related to the roles of BK channels in calcium influx and neurotransmitter release. The etiology of ID mainly involves four biological functions, including (1) presynaptic vesicle cycling and transport, (2) cytoskeleton dynamics, (3) cell-adhesion and trans-synaptic signaling and (4) protein degradation and turnover (15). Specifically, presynaptic vesicle cycling and transport determines the amount of neurotransmitter release and affects the electrical signal transmission across synapses. On rapid timescales, which are relevant to information processing, the

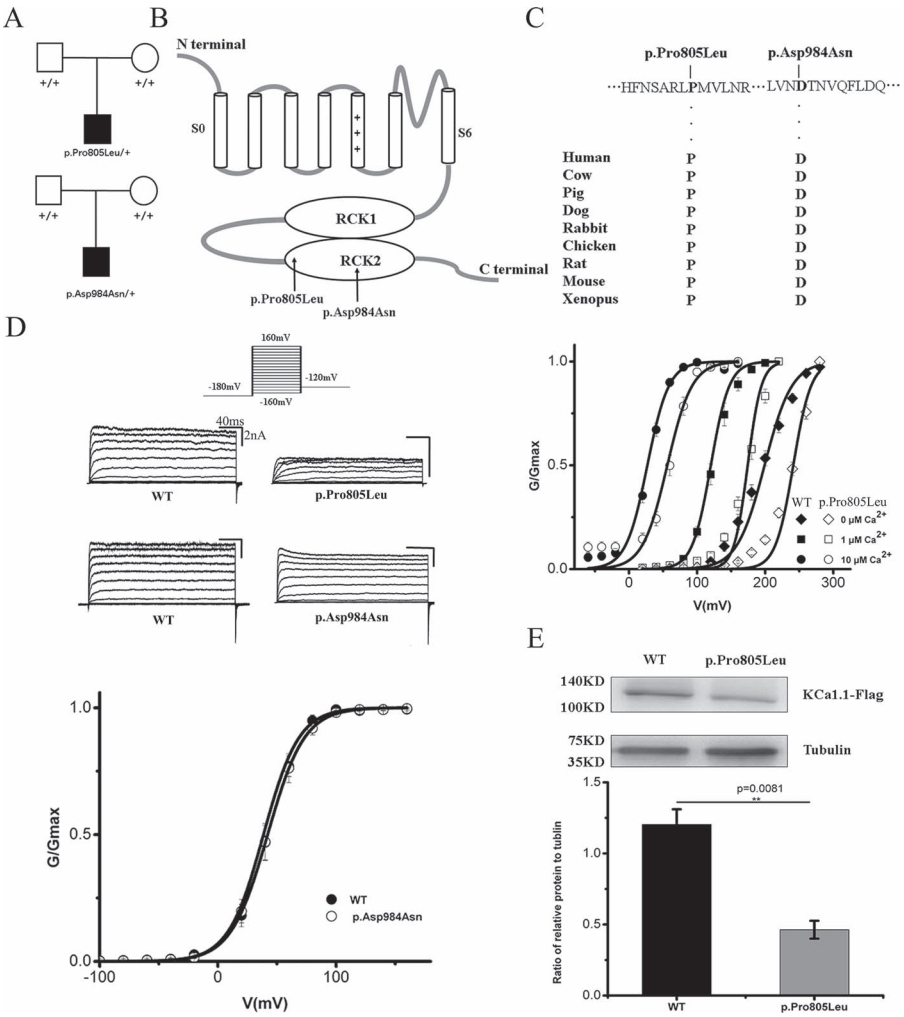

Figure 5. Identification and electrophysiological characterization of *KCNMA1* variants p.(Pro805Leu) and p.(Asp984Asn) in the RCK2 domain of the BK channel. (**A**) Pedigree structure and genotyping data for *KCNMA1* variants p.(Pro805Leu) and p.(Asp984Asn) showing the *de novo* nature of the variants. (**B**) Schematic structure of the BK channel with the location of the two variants p.(Pro805Leu) and p.(Asp984Asn) indicated by arrows. (**C**) The p.(Pro805Leu) and p.(Asp984Asn) variants occur at an evolutionally conserved amino acid residue. (**D**) Electrophysiological characterization of variants p.(Pro805Leu) and p.(Asp984Asn). Representative macroscopic currents of WT and mutant BK channels with variants p.(Pro805Leu) and p.(Asp984Asn) from inside-out patch experiments in the presence of 10 μM Ca^{2+} using the protocol indicated at the top ($n = 12–15$/group). Top right panel: the G-V curves of WT and p.(Pro805Leu) mutant BK channels are shown at nominal 0 μM Ca^{2+}, 1 μM Ca^{2+} and 10 μM Ca^{2+}. The G-V curves are fitted by Boltzmann function (solid lines) with $V_{1/2}$ and slope factor at nominal 0 μM Ca^{2+} [195.6± 15.8 mV, 25.0 ± 2.5 for WT and 238.2± 7.9 mV, 17.4 ± 2.9 for p.(Pro805Leu)], at 1 μM Ca^{2+} [124.9± 15.3 mV, 13.5 ± 3.1 for WT and 173.1 ± 12.9 mV, 15.2 ± 3.3 for p.(Pro805Leu)] and at 10 μM Ca^{2+} [27.4 ± 6.3 mV, 14.7 ± 2.1 for WT and 60.5± 9.6 mV, 15.4 ± 2.2 for p.(Pro805Leu)]. The data are presented as mean ± SEM ($n = 7–18$/group). Bottom left panel: the G-V curves of WT and p.(Asp984Asn) mutant BK channels are shown at 10 μM Ca^{2+} and fitted by Boltzmann function (solid lines) with $V_{1/2}$ and slope factor at 10 μM Ca^{2+} [41.2± 10.5 mV, 13.5 ± 1.9 for WT and 41.9± 12.6 mV, 13.7 ± 1.7 for p.(Asp984Asn)]. The data are presented as mean ± SEM ($n = 7$/group). (**e**) Western blot analysis showing the significant effect of variant p.(Pro805Leu) on the BK channel expression level ($P = 0.0081$, $n = 3$/group). Tubulin was used as a loading control.

release of neurotransmitters is predominantly determined by the shape, frequency and pattern of presynaptic action potentials (16). Action potential duration is an especially important determinant of neurotransmitter release and the amount of presynaptic calcium influx, which translates approximately into the fourth power to the release magnitude (16). Modulation of action potential duration thus represents a precise and powerful mechanism to control and regulate neurotransmitter release, which is primarily controlled by the activity of voltage-gated K+ channels (16). Furthermore, BK channels are among the major determinants of action potential duration during repetitive activity in central neurons, owing to their activation being both voltage and calcium regulated (17). In addition, BK channels are responsible for the repolarization of the action potential (17). LoF of BK channels can slow the repolarization process and prolong the action potential duration, which may increase the calcium influx and neurotransmitter release. Therefore, we hypothesize that the molecular pathogenesis of ID associated with BK channel LoF variants is mediated by abnormal neurotransmitter release.

It is also noteworthy that pathogenic *CRBN* variants associated with mild to severe ID (18,19) were thought to play a role in the assembly and surface expression of the BK channel (20,21). These pathomechanistic links underscore the association of *KCNMA1* LoF variants to ID, which can also easily be observed in the clinical presentation of the described individuals in this study.

Five of the eight patients with LoF variants in the BK channel also shared clinical features of speech delay/dysarthria/apraxia and strabismus. These findings may implicate a role of the BK

channel in neuronal control of speech and extraocular muscles or in developmental abnormalities of the same and other muscles. Collectively, the clinical data from the eight patients suggest a remarkable phenotypic variability associated with LoF variants of the BK channel. The patients carrying the p.(Gly375Arg) missense variant located in the transmembrane segment S6 present with a particularly severe phenotype including recurrent episodes of intestinal pseudoobstruction, arterial dilations and tortuosities as well as bone thickening and dysplasia. No other obvious genotype–phenotype correlation could be established between the location of variants and the presenting clinical features. The additional manifestations associated with the p.(Gly375Arg) variant could be attributed to the role of BK channels in tissues other than neurons. For instance, LoF of the BK channel was found to decrease the ability of proliferation and mineralization of osteoblasts through decreased expression of osteoblast differentiation marker genes (22). Moreover, the BK channel is also involved in smooth muscle physiology. It regulates the resting membrane potential through its activation by Ca^{2+} and hyperpolarizes plasma membranes as it does in neurons. Thus, BK channels regulate neuronal and smooth muscle excitabilities by limiting cell depolarization and contractions (23). In line with this, the BK channel is found to be a target of flavonoid naringenin, accounting for its relaxant effect on rat colonic smooth muscle contractility (23). The observed arterial dilation could be explained by *KCNMA1* expression in smooth muscle cells of the aorta (24) and its involvement in blood pressure control, although existing data are spare (25). Subsequently, other organs in which smooth muscle cell function plays a major role may be affected as well. For instance, BK channels were found to also be crucial for urinary bladder function by controlling its filling-emptying cycle (26).

We noticed a high phenotypic heterogeneity among patients carrying *KCNMA1* LoF variants (Table 1), which may be caused by variable expressivity, reduced penetrance or by the longitudinal evolution of the clinical phenotype and of different clinical features. Moreover, the p.(Asn449fs) frameshift variant was inherited from the healthy father (Fig. 3A) and thus appears to be a hypomorphic allele, which on its own is unlikely to be sufficient to cause a clinical phenotype and therefore has to occur in combination with another hypomorphic LoF variant [in our patient p.(Cys413Tyr)] to elicit a clinical presentation. These data are consistent with a previous report, which described two affected sibs with an autosomal recessive disorder consisting of generalized hypotonia, severe delayed milestones and myoclonic seizures beginning at 12 months of age. The seizures in those siblings were responsive to therapy in one and evolved to a Lennox–Gastaut pattern in the other. Brain MRI showed non-progressive severe cerebellar atrophy, vermis atrophy (more pronounced in the superior part) and slight paucity of the periventricular white matter in (12). A homozygous frameshift variant p.(Tyr676Leufs*7) was identified in the two sibs, but no functional studies were performed (12). As the heterozygous parents of these two affected sibs were healthy, the frameshift variant p.(Tyr676Leufs*7) only causes clinical disease in a homozygous but not in a heterozygous state. This raises an interesting possibility of a different pathophysiological mechanism between predicted truncating and haploinsufficient variants and missense variants. It is however also possible that some *KCNMA1* missense LoF variants confer a higher degree of penetrance by a dominant negative mechanism by impacting multiple subunits and binding proteins of the BK channel α-subunit (2,20).

Interestingly, some of the clinical features associated with the p.(Gly375Arg) variant are reminiscent of Zimmermann–Laband syndrome (ZLS), which is characterized by facial dysmorphism with gingival enlargement, hypoplasia or aplasia of nails and terminal phalanges, hypertrichosis, join hyperextensibility, hepato (spleno) megaly and ID with or without epilepsy and caused by heterozygous *de novo* gain-of-function mutations in the voltage-gated K+ channel Eag1 (Kv10.1) encoded by the *KCNH1* gene (27). The clinical features shared by ZLS and the syndrome described here to be associated with the p.(Gly375Arg) variant suggest existing interplay between Kv10.1 and BK channels in tissues where both contribute to the regulation of potassium homeostasis and current in response to stimuli.

The *KCNMA1* gene appears to harbor some hotspots for recurrent *de novo* variants. In particular, the p.(Gly375Arg) LoF variant described in this study occurred *de novo* in three independent patients (Table 1). We previously reported another *de novo* variant in *KCNMA1*, p.(Asn995Ser), which is a gain-of-function variant identified in two independent patients affected with epilepsy without paroxysmal dyskinesia (11).

Of note, *KCNMA1* knockout (KO) mice present with several abnormalities, including ataxia, weak grip, hearing loss, circadian imbalances and urinary bladder incontinence (28–31). In addition, a recent study reported slower weight gain for *KCNMA1* KO mice compared with WT littermates after weaning. Moreover, the body composition determined by quantitative magnetic resonance indicated a higher fat proportion in *KCNMA1* KO mice compared with WT littermates (32). Ataxia and weak grip in the *KCNMA1* KO mice are reminiscent of the ataxia and axial hypotonia identified in four patients with *KCNMA1* LoF variants, particularly in Patient 6 (Table 1) and in the patient carrying compound heterozygous pathogenic variants (12). Following this study, it would be interesting to determine whether *KCNMA1* KO mice also express other phenotypes present in our cohort affecting cognition/behavior, development and oral, ocular and other muscle function. Other phenotypic abnormalities such as intestinal pseudoobstruction, bone dysplasia, aortic and arterial dilations and tortuosities should be looked for in the KO mouse model.

BK channel-associated disease may be amenable to BK channel activators as BK channel LoF variants are found to abolish or markedly reduce the potassium current. Isoprimaric acid, for instance, is a BK channel activator that was found to enhance non-spatial memory in mice with Alzheimer's disease and restore the basic synapse transmission and long-term potentiation (3,33). BK channel opener BMS-205352 was found to restore hippocampal glutamate homeostasis and treat abnormalities in social recognition and interaction, non-social anxiety and spatial memory in *FMR1* KO mice (34). BMS-205352 was also found to restore impaired habituation associated with some psychiatric disorders (35). Evaluation of the therapeutic potential of these compounds and other BK channel activators in appropriate *KCNMA1* animal models and eventually in human patients with LoF variants of BK channels would be of clinical interest. Similarly, strategies aimed to increase the function or activity of the WT allele of *KCNMA1* in heterozygous carriers by enhancing trafficking of the WT allele to the cell surface or its stability could have therapeutic potential. Obviously, gene therapy to correct the disease-causing variants using various technologies such as CRISPR-Cas9-based gene editing may also be considered for treatment of patients with LoF variants in BK channels.

In summary, we identified and functionally characterized eight different LoF variants in the BK channel [p.(Ser351Tyr),

p.(Gly356Arg), p.(Gly375Arg), p.(Asn449fs), p.(Cys413Tyr), p.(Ile663Val), p.(Pro805Leu) and p.(Asp984Asn)] affecting nine patients and demonstrated that impairment of BK channel function is associated with a variable phenotypic presentation ranging from ID and developmental delay alone to ataxia, axial hypotonia, apraxia/dysarthria/speech delay, cerebral atrophy, strabismus and dysmorphism. Our report substantially expands the spectrum of clinical phenotypes and diseases associated with BK channel variants.

Materials and Methods

WES, WGS and study subjects

Whole exome sequencing (WES) and data analyses were performed as previously described (37–39). Whole genome sequencing (WGS) was performed using the Illumina HiSeq X sequencing platform with an average 40× coverage (37–39). Sequence variants were uploaded to a custom analysis software application called Codicem for interpretation. Observed variants of interest were confirmed using an orthogonal sequencing technology [Sanger (dideoxy) sequencing]. The p.(Ser351Tyr) variant was identified by WGS while all other *KCNMA1* variants were identified by WES. All *KCNMA1* variants were annotated based on the GenBank transcript NM_002247.3. This study was approved by the Institutional Review Board (IRB) on Human Subject Research at the Cleveland Clinic, the Ethics Committee on Human Subject Research at Huazhong University of Science and Technology and other local IRBs. Written informed consent was obtained from all study subjects according to the appropriate IRB policies. The study abides by the Declaration of Helsinki principles.

Plasmids and mutagenesis

The expression plasmid for FLAG-tagged *KCNMA1* (GenBank accession number U23767), *KCNMA1*-pcDNA3.1, was described previously (11). Mutations were generated in the *KCNMA1*-pcDNA3.1 plasmid using polymerase chain reaction–based site-directed mutagenesis and verified by direct DNA sequence analysis as described by us previously (40,41).

Cell culture and transfection

HEK293T cells were cultured on coverslips in 24-well plates with Dulbecco's Modified Eagle Medium (DMEM) (Gibco, Gaithersburg, MD) supplemented with 10% fetal bovine serum (Gibco, Gaithersburg, MD) at 37°C and 5% CO_2. HEK293T were co-transfected with either the WT or mutant *KCNMA1* expression plasmid and the pEGFP-N1 plasmid using Lipofectamine 2000 (Invitrogen, Carlsbad, CA). The transfected cells showing a green EGFP signal (marker for successful transfection) were selected for patch-clamp recordings.

Western blot analysis

HEK293T cells were transfected with either the WT or mutant *KCNMA1* expression plasmid as described above, lysed and used for western blot analysis using an anti-FLAG antibody (MBL, Woburn, MA) as described previously (36).

Patch-clamp recording

Electrophysiological experiments were performed using a patch-clamping work station with a Multiclamp 700B amplifier and a 1440A Digital Analog Converter (Axon Instruments, San Jose, CA). All data was collected using the Pclamp software as described (1,11,40). Recorded data were analyzed with Clampfit (Axon Instruments, San Jose, CA), Origin 8.5 and SigmaPlot (SPSS) software programs as described previously (1,11,40). Patch-clamp recordings were carried out 24 h after transfection. The experiments were performed at room temperatures (22–25°C). After a GΩ seal was established, the pipette was moved to drag the patch from the cell membrane. All recordings were carried out with inside-out configuration. The patch pipettes were made of borosilicate glass capillaries and pulled with a P-97 instrument (Sutter Instrument, Novato, CA). The resistances of the patch pipettes were 3–5 MΩ when filled with the pipette solution. The recordings were digitized at 50 kHz and low-pass-filtered at 5 kHz. During the recordings, solutions with different concentrations of calcium were applied onto the patches by gravity via a perfusion pipette containing eight solution channels. The solutions used for patch clamping included the following:

- Pipette solution containing the following (in mM): 160 $MeSO_3K$, 2 $MgCl_2$ and 10 HEPES.
- Nominal 0 μM Ca^{2+} solution containing the following (in mM): 160 $MeSO_3K$, 5 EGTA and 10 HEPES.
- 1 μM Ca^{2+} solution containing the following (in mM): 160 $MeSO_3K$, 5 EGTA, 3.25 $CaCl_2$ and 10 HEPES.
- 10 μM Ca^{2+} solution containing the following (in mM): 160 $MeSO_3K$, 5 HEDTA, 2.988 $CaCl_2$ and 10 HEPES.

Statistical analysis

A two-tailed Student's *t*-test was used for determination of statistically significant differences. Data are shown as mean ± standard deviation (SD) or mean ± standard error of mean (SEM) as noted in the text. A *P*-value of 0.05 or less was considered to be statistically significant.

Supplementary Material

Supplementary Material is available at *HMG* online.

Acknowledgements

We thank Gang Yu for the analysis of the variant p.(Ile663Val) against the 3D structure of the BK channel and members of the Wang laboratory and the Center for Human Genome Research for scientific discussions and assistance.

Conflict of Interest statement. None declared.

Funding

National Natural Science Foundation of China (31430047); Hubei Province's Innovative Team (2017CFA014); National Institutes of Health/National Heart, Lung and Blood Institute (R01 HL121358 and R01 HL126729).

Author contributions

Experimental design: Q.K.W., G.M.S.M., Q.C. and A.V.; clinical studies and data analysis: A.V., G.M.S.M., S.M., S.A.S.V., B.I., A.S.M., A.C.E.H., O.B., J.T., C.H., B.C., B.G., A.R., S.N., D.L., Y.D., C.T.R., L. F., S. B, L.D., D.H. and D.B; basic experiments and data analysis: L.L., X.L., Y.H., C.X., Q.C. and Q.K.W.; draft of manuscript: L.L., X.L., Y.H., Q.C., A.V. and Q.K.W.; revision of manuscript: all

authors; project supervision: Q.K.W., G.M.S.M., Q.C. and A.V.; approval of submission: all authors.

References

1. Du, W., Bautista, J.F., Yang, H., Diez-Sampedro, A., You, S.A., Wang, L., Kotagal, P., Luders, H.O., Shi, J., Cui, J. *et al* (2005) Calcium-sensitive potassium channelopathy in human epilepsy and paroxysmal movement disorder. *Nat. Genet.*, **37**, 733–738.
2. Latorre, R., Castillo, K., Carrasquel-Ursulaez, W., Sepulveda, R.V., Gonzalez-Nilo, F., Gonzalez, C. and Alvarez, O. (2017) Molecular determinants of BK channel functional diversity and functioning. *Physiol. Rev.*, **97**, 39–87.
3. Kshatri, A.S., Gonzalez-Hernandez, A. and Giraldez, T. (2018) Physiological roles and therapeutic potential of Ca^{2+} activated potassium channels in the nervous system. *Front. Mol. Neurosci.*, **11**, 258.
4. Petersen, O.H. and Maruyama, Y. (1984) Calcium-activated potassium channels and their role in secretion. *Nature*, **307**, 693–696.
5. Robitaille, R. and Charlton, M.P. (1992) Presynaptic calcium signals and transmitter release are modulated by calcium-activated potassium channels. *J. Neurosci.*, **12**, 297–305.
6. Murrow, B.W. and Fuchs, P.A. (1990) Preferential expression of transient potassium current (IA) by 'short' hair cells of the chick's cochlea. *Proc. Biol. Sci.*, **242**, 189–195.
7. Brayden, J.E. and Nelson, M.T. (1992) Regulation of arterial tone by activation of calcium-dependent potassium channels. *Science*, **256**, 532–535.
8. Wu, Y.C., Ricci, A.J. and Fettiplace, R. (1999) Two components of transducer adaptation in auditory hair cells. *J. Neurophysiol.*, **82**, 2171–2181.
9. Zhang, Y.Y., Yue, J., Che, H., Sun, H.Y., Tse, H.F. and Li, G.R. (2014) BKCa and hEag1 channels regulate cell proliferation and differentiation in human bone marrow-derived mesenchymal stem cells. *J. Cell. Physiol.*, **229**, 202–212.
10. Maqoud, F., Curci, A., Scala, R., Pannunzio, A., Campanella, F., Coluccia, M., Passantino, G., Zizzo, N. and Tricarico, D. (2018) Cell cycle regulation by Ca^{2+}-activated K^{+} (BK) channels modulators in SH-SY5Y neuroblastoma cells. *Int. J. Mol. Sci.*, **19**, 2442.
11. Li, X., Poschmann, S., Chen, Q., Fazeli, W., Oundjian, N.J., Snoeijen-Schouwenaars, F.M., Fricke, O., Kamsteeg, E.J., Willemsen, M. and Wang, Q.K. (2018) De novo BK channel variant causes epilepsy by affecting voltage gating but not Ca^{2+} sensitivity. *Eur. J. Hum. Genet.*, **26**, 220–229.
12. Tabarki, B., AlMajhad, N., AlHashem, A., Shaheen, R. and Alkuraya, F.S. (2016) Homozygous KCNMA1 mutation as a cause of cerebellar atrophy, developmental delay and seizures. *Hum. Genet.*, **135**, 1295–1298.
13. Zhang, Z.B., Tian, M.Q., Gao, K., Jiang, Y.W. and Wu, Y. (2015) De novo KCNMA1 mutations in children with early-onset paroxysmal dyskinesia and developmental delay. *Mov. Disord.*, **30**, 1290–1292.
14. Sobreira, N., Schiettecatte, F., Valle, D. and Hamosh, A. (2015) GeneMatcher: a matching tool for connecting investigators with an interest in the same gene. *Hum. Mutat.*, **36**, 928–930.
15. Srivastava, A.K. and Schwartz, C.E. (2014) Intellectual disability and autism spectrum disorders: causal genes and molecular mechanisms. *Neurosci. Biobehav. Rev.*, **46**, 161–174.
16. Bean, B.P. (2007) The action potential in mammalian central neurons. *Nat. Rev. Neurosci.*, **8**, 451–465.
17. Salkoff, L., Butler, A., Ferreira, G., Santi, C. and Wei, A. (2006) High-conductance potassium channels of the SLO family. *Nat. Rev. Neurosci.*, **7**, 921–931.
18. Sheereen, A., Alaamery, M., Bawazeer, S., Al Yafee, Y., Massadeh, S. and Eyaid, W. (2017) A missense mutation in the CRBN gene that segregates with intellectual disability and self-mutilating behaviour in a consanguineous Saudi family. *J. Med. Genet.*, **54**, 236–240.
19. Higgins, J.J., Pucilowska, J., Lombardi, R.Q. and Rooney, J.P. (2004) A mutation in a novel ATP-dependent Lon protease gene in a kindred with mild mental retardation. *Neurology*, **63**, 1927–1931.
20. Jo, S., Lee, K.H., Song, S., Jung, Y.K. and Park, C.S. (2005) Identification and functional characterization of cereblon as a binding protein for large-conductance calcium-activated potassium channel in rat brain. *J. Neurochem.*, **94**, 1212–1224.
21. Higgins, J.J., Hao, J., Kosofsky, B.E. and Rajadhyaksha, A.M. (2008) Dysregulation of large-conductance Ca2+−activated K+ channel expression in nonsyndromal mental retardation due to a cereblon p.R419X mutation. *Neurogenetics*, **9**, 219–223.
22. Hei, H., Gao, J., Dong, J., Tao, J., Tian, L., Pan, W., Wang, H. and Zhang, X. (2016) BK knockout by TALEN-mediated gene targeting in osteoblasts: KCNMA1 determines the proliferation and differentiation of osteoblasts. *Mol. Cells*, **39**, 530–535.
23. Yang, Z., Pan, A., Zuo, W., Guo, J. and Zhou, W. (2014) Relaxant effect of flavonoid naringenin on contractile activity of rat colonic smooth muscle. *J. Ethnopharmacol.*, **155**, 1177–1183.
24. Gueguinou, M., Chantome, A., Fromont, G., Bougnoux, P., Vandier, C. and Potier-Cartereau, M. (2014) KCa and Ca(2+) channels: the complex thought. *Biochim. Biophys. Acta*, **1843**, 2322–2333.
25. Kohler, R., Kaistha, B.P. and Wulff, H. (2010) Vascular KCa-channels as therapeutic targets in hypertension and restenosis disease. *Expert Opin. Ther. Targets*, **14**, 143–155.
26. Petkov, G.V. (2014) Central role of the BK channel in urinary bladder smooth muscle physiology and pathophysiology. *Am. J. Physiol. Regul. Integr. Comp. Physiol.*, **307**, R571–R584.
27. Kortum, F., Caputo, V., Bauer, C.K., Stella, L., Ciolfi, A., Alawi, M., Bocchinfuso, G., Flex, E., Paolacci, S., Dentici, M.L. *et al.* (2015) Mutations in KCNH1 and ATP6V1B2 cause Zimmermann–Laband syndrome. *Nat. Genet.*, **47**, 661–667.
28. Sausbier, M., Hu, H., Arntz, C., Feil, S., Kamm, S., Adelsberger, H., Sausbier, U., Sailer, C.A., Feil, R., Hofmann, F. *et al.* (2004) Cerebellar ataxia and Purkinje cell dysfunction caused by Ca2+-activated K+ channel deficiency. *Proc. Natl. Acad. Sci. USA*, **101**, 9474–9478.
29. Meredith, A.L., Thorneloe, K.S., Werner, M.E., Nelson, M.T. and Aldrich, R.W. (2004) Overactive bladder and incontinence in the absence of the BK large conductance Ca2+-activated K+ channel. *J. Biol. Chem.*, **279**, 36746–36752.
30. Meredith, A.L., Wiler, S.W., Miller, B.H., Takahashi, J.S., Fodor, A.A., Ruby, N.F. and Aldrich, R.W. (2006) BK calcium-activated potassium channels regulate circadian behavioral rhythms and pacemaker output. *Nat. Neurosci.*, **9**, 1041–1049.
31. Ruttiger, L., Sausbier, M., Zimmermann, U., Winter, H., Braig, C., Engel, J., Knirsch, M., Arntz, C., Langer, P., Hirt, B. *et al.* (2004) Deletion of the Ca2+-activated potassium (BK) alpha-subunit but not the BKbeta1-subunit leads to progressive hearing loss. *Proc. Natl. Acad. Sci. U. S. A.*, **101**, 12922–12927.
32. Halm, S.T., Bottomley, M.A., Almutairi, M.M., Di Fulvio, M. and Halm, D.R. (2017) Survival and growth of C57BL/6J mice lacking the BK channel, Kcnma1: lower adult body weight

occurs together with higher body fat. *Physiol. Rep.*, **5**, pii: e13137.
33. Wang, L., Kang, H., Li, Y., Shui, Y., Yamamoto, R., Sugai, T. and Kato, N. (2015) Cognitive recovery by chronic activation of the large-conductance calcium-activated potassium channel in a mouse model of Alzheimer's disease. *Neuropharmacology*, **92**, 8–15.
34. Hebert, B., Pietropaolo, S., Meme, S., Laudier, B., Laugeray, A., Doisne, N., Quartier, A., Lefeuvre, S., Got, L., Cahard, D. *et al.* (2014) Rescue of fragile X syndrome phenotypes in Fmr1 KO mice by a BKCa channel opener molecule. *Orphanet. J. Rare Dis.*, **9**, 124.
35. Zaman, T., De Oliveira, C., Smoka, M., Narla, C., Poulter, M.O. and Schmid, S. (2017) BK channels mediate synaptic plasticity underlying habituation in rats. *J. Neurosci.*, **37**, 4540–4551.
36. Chakrabarti, S., Wu, X., Yang, Z., Wu, L., Yong, S.L., Zhang, C., Hu, K., Wang, Q.K. and Chen, Q. (2013) MOG1 rescues defective trafficking of Na(v)1.5 mutations in Brugada syndrome and sick sinus syndrome. *Circ. Arrhythm. Electrophysiol.*, **6**, 392–401.
37. Thevenon, J., Duffourd, Y., Masurel-Paulet, A., Lefebvre, M., Feillet, F., El Chehadeh-Djebbar, S., St-Onge, J., Steinmetz, A., Huet, F., Chouchane, M. *et al.* (2016) Diagnostic odyssey in severe neurodevelopmental disorders: toward clinical whole-exome sequencing as a first-line diagnostic test. *Clin. Genet.*, **89**, 700–707.
38. Wang, C., Wu, M., Qian, J., Li, B., Tu, X., Xu, C., Li, S., Chen, S., Zhao, Y., Huang, Y. *et al.* (2016) Identification of rare variants in TNNI3 with atrial fibrillation in a Chinese GeneID population. *Mol. Genet. Genomics*, **291**, 79–92.
39. Li, S., Xi, Q., Zhang, X., Yu, D., Li, L., Jiang, Z., Chen, Q., Wang, Q.K. and Traboulsi, E.I. (2018) Identification of a mutation in CNNM4 by whole exome sequencing in an Amish family and functional link between CNNM4 and IQCB1. *Mol. Genet. Genomics*, **293**, 699–710.
40. Chen, Q., Kirsch, G.E., Zhang, D., Brugada, R., Brugada, J., Brugada, P., Potenza, D., Moya, A., Borggrefe, M., Breithardt, G. *et al.* (1998) Genetic basis and molecular mechanism for idiopathic ventricular fibrillation. *Nature*, **392**, 293–296.
41. Zhang, X., Chen, S., Yoo, S., Chakrabarti, S., Zhang, T., Ke, T., Oberti, C., Yong, S.L., Fang, F., Li, L. *et al.* (2008) Mutation in nuclear pore component NUP155 leads to atrial fibrillation and early sudden cardiac death. *Cell*, **135**, 1017–1027.